

# Microstructure Evolution and Mechanical Properties of ZM81-xSn Wrought Magnesium Alloys

Qi Fugang<sup>1,2</sup>, Luo Wenzhong<sup>2</sup>, Wu Chuanping<sup>1</sup>, Zhao Nie<sup>1,2</sup>, Ye Zhisong<sup>2</sup>  
Hou Caihong<sup>1</sup>, Zhang Dingfei<sup>3</sup>

<sup>1</sup> State Key Laboratory of Disaster Prevention and Reduction for Power Grid Transmission and Distribution Equipment, Changsha 410000, China; <sup>2</sup> Xiangtan University, Xiangtan 411105, China; <sup>3</sup> Chongqing University, Chongqing 400045, China

**Abstract:** The microstructure and mechanical properties of the ZM81 alloys with various Sn contents after extrusion and T6 treatments were investigated by OM, XRD, SEM, TEM, hardness test and uniaxial tensile test at room temperature. The results show that after the addition of Sn element, an Mg<sub>2</sub>Sn eutectic phase is formed, which can refine the as-cast microstructure. Sn element has an obvious effect on refining the microstructure of as-extruded alloys by restricting the occurrence of dynamic recrystallization and restraining the grain growth during extrusion, and improves the mechanical properties. T6 treatments, especially the double aging, can significantly increase the strength of the extruded alloys. Among them, the ZM81-4Sn alloy with double aging exhibits an ultimate tensile strength of 416 MPa, a 0.2% yield strength of 393 MPa and an elongation of 4.1%. The microstructure characterization suggests that the high strength of the peak-aged alloys is attributed to the combined precipitation strengthening of the fine and dispersed MgZn<sub>2</sub> and Mg<sub>2</sub>Sn precipitates, and the precipitates after double peak aging are finer than those after single peak aging.

**Key words:** ZM81 alloy; Sn; precipitate; mechanical properties

As the lightest structural metal materials, magnesium (Mg) alloys have great potential for weight reduction of automobiles and other transportation vehicles<sup>[1]</sup>. However, the application of Mg alloys is still restricted due to their inadequate strength, poor formability, and high cost of expensive composition elements used and/or special processing technology involved<sup>[2]</sup>. Therefore, it is necessary to develop some new wrought Mg alloys with high strength and low-cost to further broaden the application of Mg alloys.

Mg-Zn system alloys are the most widely used wrought Mg alloys, which have a more pronounced response to age hardening compared to other Mg alloys<sup>[3,4]</sup>. Recently, as a new promising high-strength Mg alloy, Mg-6Zn-1Mn (wt%, ZM61) alloy has attracted attention due to its good castability, excellent formability and significant precipitation hardening response<sup>[5-7]</sup>. In our previous study, it is reported

that ZM61 alloy with double aging (high temperature aging after pre-aging at a lower temperature) after solution treatment exhibits higher strengths than single aged alloy. In this study, the microstructure and mechanical properties of Mg-xZn-1Mn (x=4, 5, 6, 7, 8, 9, wt%) alloy were investigated and it is found that Mg-8Zn-1Mn (ZM81) alloy exhibits the highest tensile properties<sup>[6]</sup>.

In addition, the Mg-Sn alloy is known as a precipitation-hardening system due to the formation of Mg<sub>2</sub>Sn precipitates (fcc,  $a=0.676$  nm, point group  $m\bar{3}m$ )<sup>[8,9]</sup>. However, the precipitation hardening response in the binary alloy is low because the Mg<sub>2</sub>Sn precipitates form with a lath-shaped morphology on the (0001)<sub>Mg</sub> basal planes of the matrix<sup>[8,10]</sup>. Sasaki et al<sup>[11]</sup> reported that a minor addition of Zn can enhance the age-hardening response of the binary alloy through homogeneous dispersion of the precipitates.

Received date: March 22, 2019

Foundation item: National Natural Science Foundation of China (51701172); Natural Science Foundation of Hunan Province (2018JJ3504); China Postdoctoral Science Foundation (2018M632977); State Key Laboratory Opening Foundation of Disaster Prevention and Reduction for Power Grid Transmission and Distribution Equipment (2016ZKFW127)

Corresponding author: Qi Fugang, Ph. D., Associate Professor, School of Materials Science and Engineering, Xiangtan University, Xiangtan 411105, P. R. China, Tel: 0086-731-58298119, E-mail: qifugang@xtu.edu.cn

Copyright © 2020, Northwest Institute for Nonferrous Metal Research. Published by Science Press. All rights reserved.

Since the Zn content is too low, it may be difficult to give full play to precipitation strengthening effect of MgZn<sub>2</sub> phase. Recently, some researches on the alloying and heat treatment of highly alloyed Mg-Sn-Zn based alloys have been reported<sup>[11-14]</sup>. Based on the previous researches by our research group<sup>[6, 12]</sup>, it is of great interest to research the microstructure and mechanical properties of the ZM81 alloys with different Sn contents. Therefore, in the present study, the effects of Sn addition on the microstructure and mechanical properties of ZM81 alloy were investigated.

## 1 Experiment

The alloy ingots with a nominal composition of ZM81-xSn (x=0, 2, 4, 6, 8, 10, wt%) were prepared by commercial purity Mg (>99.9%), pure Zn (>99.95%), pure Sn (>99.9%) and Mg-4.1%Mn master alloy. All the materials added were melted in a steel crucible inside an electrical resistance furnace under a SO<sub>2</sub>+CO<sub>2</sub> protective gas and then cast into a steel mold. The chemical compositions were analyzed by XRF-800 CCDE X-ray fluorescence spectrometer and the result is shown in Table 1. The ingots were then homogenized at 330°C for 24 h followed by air cooling. The homogenized ingots were extruded at 330 °C with an extrusion ratio of 25 and a ram speed of 2 mm/s. Then the extruded bars were solution-treated at 400 °C for 3 h followed by water quenching (T4). After solution treatment, the following artificial aging treatments (T6) would be divided into single aging and double aging. The single aging was carried out at 180 °C until peak hardness was reached. The double aging was carried out by pre-aging at 90 °C for 24 h, followed by the second aging at 180 °C until peak hardness was reached.

Hardness measurements were performed by a micro-Vickers apparatus under a load of 50 g. The mechanical properties of the as-extruded and peak-aged samples were evaluated by tensile tests at room temperature. The tensile tests were conducted on a Sans CMT-5105 electronic universal testing machine at room temperature with a cross-head speed of 3 mm/min.

**Table 1 Chemical composition of the test alloys**

Nominal alloy	Actual composition/wt%			
	Mg	Zn	Mn	Sn
ZM81	Bal.	7.86	0.96	—
ZM81-2Sn	Bal.	7.42	1.02	2.19
ZM81-4Sn	Bal.	7.68	0.91	4.09
ZM81-6Sn	Bal.	7.62	1.03	6.15
ZM81-8Sn	Bal.	7.67	0.98	8.37
ZM81-10Sn	Bal.	7.64	0.97	9.72

Microstructure was characterized by optical microscopy (OM), scanning electron microscopy (SEM) and transmission electron microscopy (TEM). The SEM observation was performed by a TESCAN VEGA II scanning electron microscope equipped with an Oxford INCA Energy 350 energy dispersive X-ray spectrometer (EDS). The TEM observation was carried out using a Zeiss LIBRA 200 FE equipped with an EDS detector. Phase constitution was determined by a Rigaku D/max 2500PC X-ray diffractometer (XRD) using a Cu K $\alpha$  radiation with a scanning angle from 10° to 90° and a scanning rate of 4°/min.

## 2 Results and Discussion

### 2.1 As-cast microstructure

Fig.1 shows the optical microstructures of the as-cast alloys. It can be seen that the as-cast microstructure consists of coarse  $\alpha$ -Mg dendrites, interdendritic and eutectic compounds between dendrite arms. As the Sn content increases, the volume fraction of the eutectic compounds increases gradually, and the dendrites are refined. The XRD spectra of the as-cast alloy are shown in Fig.2. It can be seen that the phase components of ZM81 alloy are mainly  $\alpha$ -Mg matrix, Mg<sub>7</sub>Zn<sub>3</sub> phase and Mn phase. When Sn element is added to the ZM81 alloy, a new Mg<sub>2</sub>Sn phase is formed, and as the amount of Sn added increases, the diffraction peak of the Mg<sub>2</sub>Sn phase increases, that is, the volume fraction of this phase increases.

Fig.3 shows the backscattered electron (BSE) images of ZM81, ZM81-4Sn and ZM81-8Sn alloys. For the ZM81 alloy, based on the OM and SEM analysis, it can be known that the interdendritic compounds are mainly Mg-Zn phase, and it can be further confirmed by the XRD results (Fig.2) that they are mainly the Mg<sub>7</sub>Zn<sub>3</sub> eutectic phase. When Sn element is added to the ZM81 alloy, it can be seen from Fig.2 that the eutectic compound clearly exhibits two colors of black and white, which can be presumed to be two phases. It can be further confirmed from Fig.3 that the eutectic compound is indeed two phases. The EDS analysis shows that the bright white parts in Fig.3b and 3c are mainly composed of Mg and Sn, and its atomic ratio is about 2:1, which can be presumed to be Mg<sub>2</sub>Sn eutectic phase. The slightly darker parts are mainly composed of Mg, Zn and Mn. The atomic ratio of Mg to Zn is about 7:3, which is presumed to be the Mg<sub>7</sub>Zn<sub>3</sub> eutectic phase.

### 2.2 As-extruded microstructure

The main purpose of the homogenization treatment before extrusion is mainly to improve the structural non-uniformity of the ingot and greatly reduce the deformation resistance of the alloy. Fig.4 shows the optical micrographs of the as-homogenized alloys. It can be seen that after the homogenization treatment, some eutectic compounds are dissolved, but the black eutectic compounds are not dissolved. As the Sn content increases, the black phases

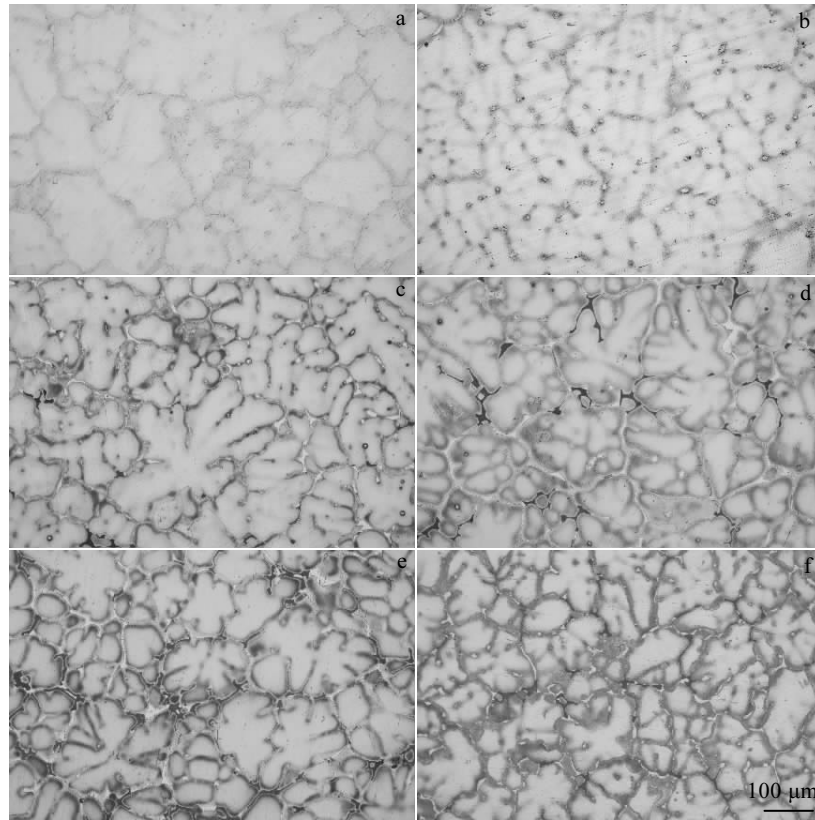


Fig.1 Optical micrographs of the as-cast ZM81-xSn alloys: (a) x=0, (b) x=2, (c) x=4, (d) x=6, (e) x=8, and (f) x=10

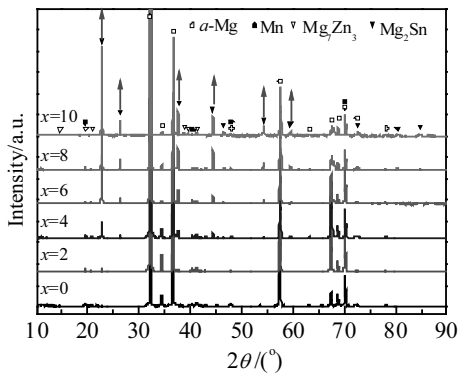


Fig.2 XRD patterns of the as-cast ZM81-xSn alloys (red arrows in the figure indicate the intensifying tendency of  $Mg_2Sn$  phase diffraction peak)

increase, which are the  $Mg_2Sn$  eutectic phases. Fig.5 shows the BSE images of the as-homogenized ZM81, ZM81-4Sn and ZM81-8Sn alloys. For the ZM81 alloy, the bulk Mg-Zn eutectic compounds are substantially dissolved after homogenization. However, for the Sn-containing alloy, the white bright  $Mg_2Sn$  eutectic phases cannot be dissolved into the matrix after homogenization. Thus, it can be concluded that the homogenization treatment at 330 °C for 24 h can

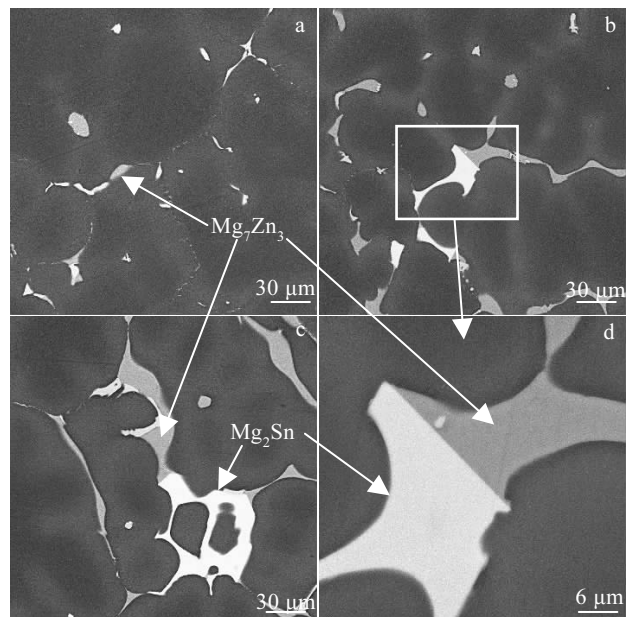


Fig.3 BSE micrographs of as-cast alloys: (a) ZM81, (b, d) ZM81-4Sn, and (c) ZM81-8Sn

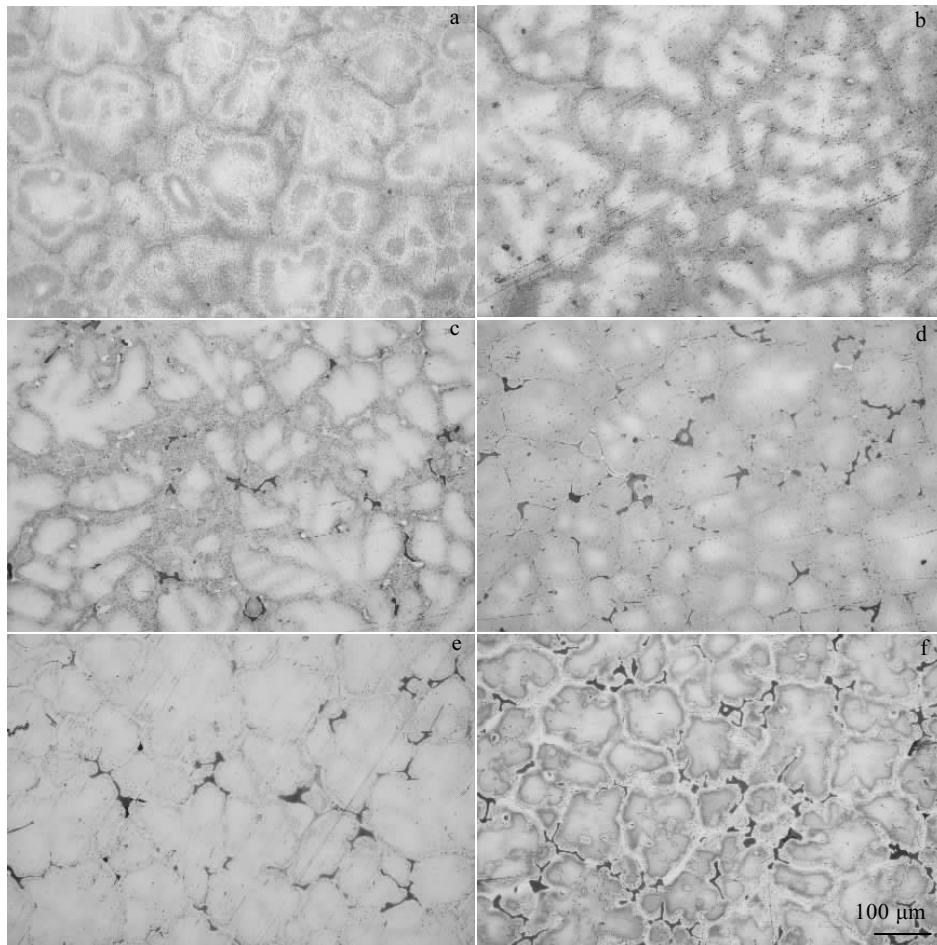


Fig.4 Optical micrographs of the as-homogenized ZM81-xSn alloys: (a)  $x=0$ , (b)  $x=2$ , (c)  $x=4$ , (d)  $x=6$ , (e)  $x=8$ , and (f)  $x=10$

only cause the dissolution of the  $Mg_7Zn_3$  eutectic phase, but cannot affect the morphology of  $Mg_2Sn$  phase due to its high temperature stability<sup>[15]</sup>.

Fig.6 shows the optical micrographs of the as-extruded alloys taken parallel to the extrusion direction. For the ZM81 alloy, the dynamic recrystallization (DRX) during the extrusion process is relatively sufficient, and the recrystallized grain size is relatively uniform, with an average grain size of about 7  $\mu m$ . With the Sn addition, the microstructure of the as-extruded alloy is transformed into a duplex grain structure, that is, there are many unrecrystallized grains in the microstructure. As the Sn content increases, the grain size of the recrystallized microstructure gradually decreases, the extrusion streamlines are more and more obvious, and the recrystallized grains at the streamline are very small. According to the XRD analysis (Fig.7), it can be known that the bulk compounds and particles constituting the streamline are undissolved  $Mg_2Sn$  and residual  $Mg_7Zn_3$  eutectic phase.

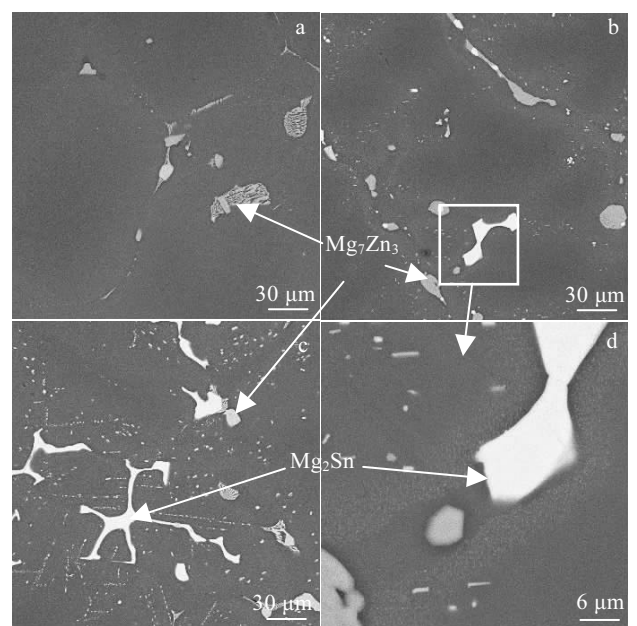


Fig.5 BSE micrographs of the as-homogenized alloys: (a) ZM81, (b, d) ZM81-4Sn, and (c) ZM81-8Sn

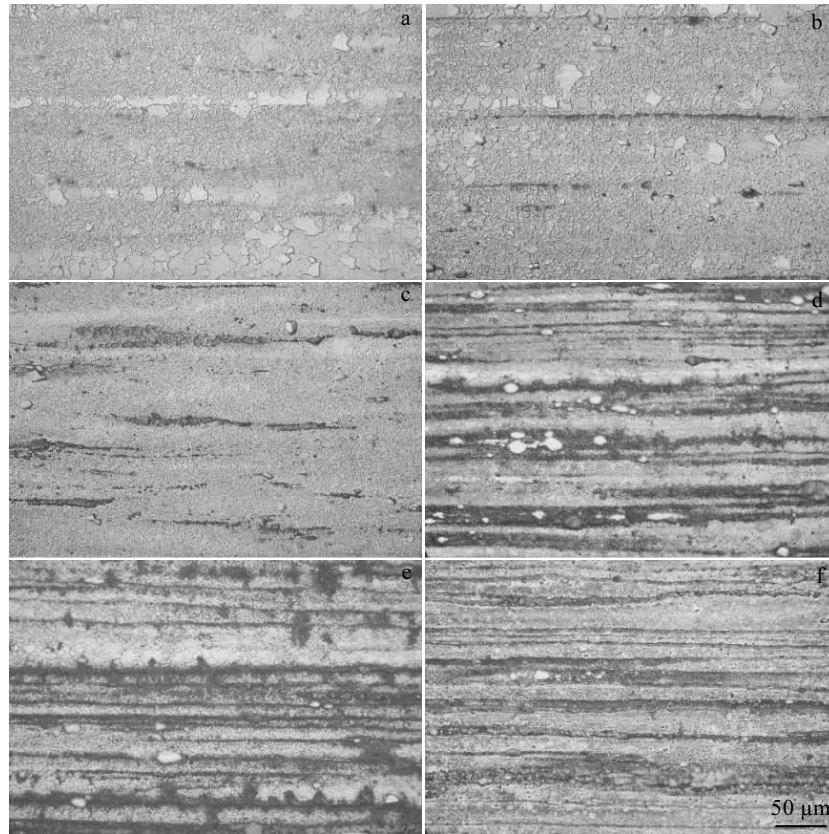


Fig.6 Optical micrographs of the as-extruded ZM81- $x$ Sn alloys taken parallel to the extrusion direction: (a)  $x=0$ , (b)  $x=2$ , (c)  $x=4$ , (d)  $x=6$ , (e)  $x=8$ , and (f)  $x=10$

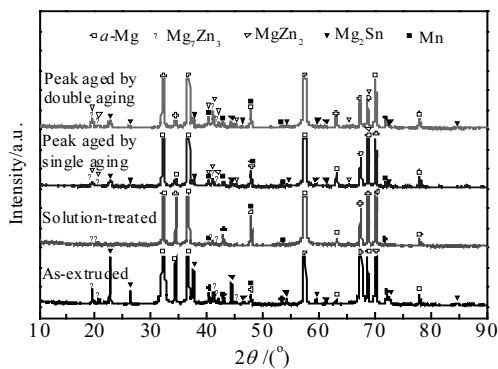


Fig.7 XRD patterns of the ZM81-4Sn alloys in different states

### 2.3 Age-hardening response

Fig.8 shows the optical micrographs of the solution-treated alloys. For ZM81 alloy, the compounds and particles at the streamlines in the as-extruded structures are mostly dissolved in the matrix, resulting in a high zinc solid solution concentration. According to the Mg-Zn phase diagram<sup>[16]</sup>, the maximum solubility of Zn in Mg is about 6.2%, so a very small amount of undissolved  $Mg_7Zn_3$

phases are still remained in the alloys, as illustrated by SEM image in Fig.9a. When the Sn content does not exceed 4 wt%, the solid solution effect is still good, and the matrix has almost no residual bulk second phase particles. For the ZM81-4Sn alloy, almost all the broken compounds are dissolved into the matrix except for a very small amount of the residual  $Mg_7Zn_3$  phases. The XRD pattern of solution-treated ZM81-4Sn alloy is shown in Fig.7. It is obvious that the solution-treated sample consists of  $\alpha$ -Mg, Mn and  $Mg_7Zn_3$  phases. With the further increase of the Sn content, the undissolved second phase particles increase and the size increases, and it is presumed that most of the residual second phases are  $Mg_2Sn$  and  $Mg_7Zn_3$  phases.

Fig.10 shows the aging curves of the solution-treated ZM81- $x$ Sn alloys subjected to single aging at 180 °C and double aging at 180 °C (pre-aging at 90 °C for 24 h). During the single aging at 180 °C, the hardness of the ZM81-4Sn alloy increases with aging time and reaches the peak harnesses (810 MPa) after 12 h. A significant increase in the hardness of ZM81-4Sn is observed after double aging and the time to reach the peak hardness (920 MPa) of 6 h is significantly shorter than 12 h for single aging. In addition, the age-hardening behavior of double aged ZM81- $x$ Sn alloys suggests that the peak hardness values gradually

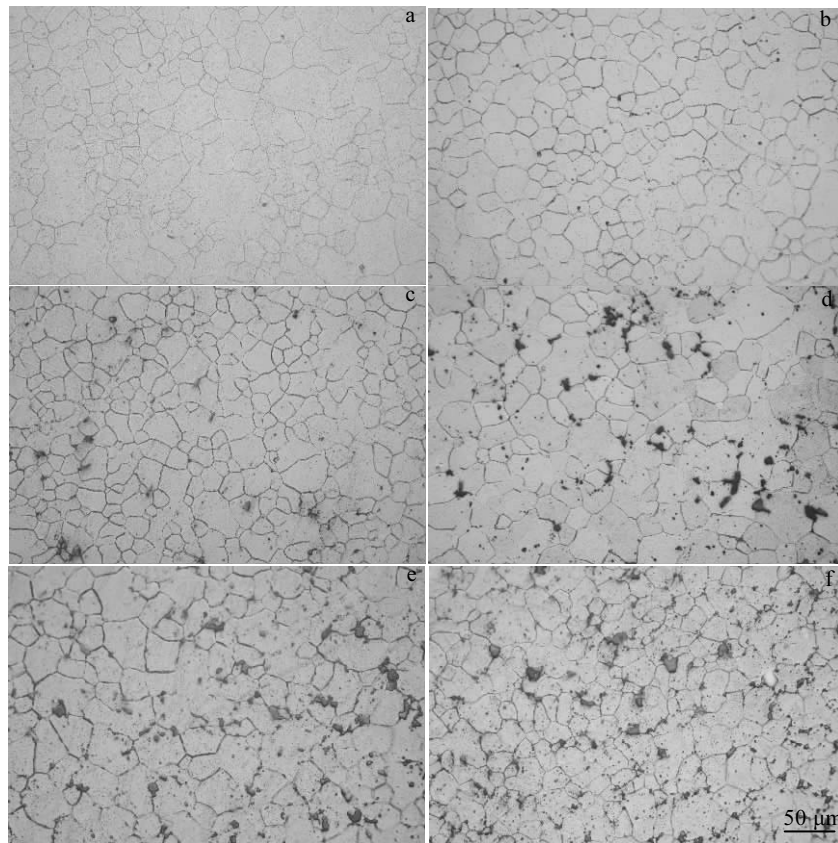


Fig.8 Optical micrographs of the solution-treated ZM81-xSn alloys taken perpendicular to the extrusion direction: (a) x=0, (b) x=2, (c) x=4, (d) x=6, (e) x=8, and (f) x=10

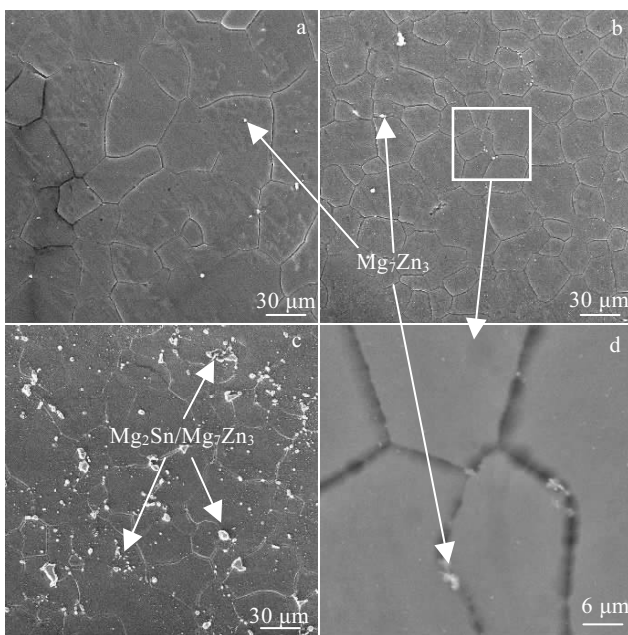


Fig.9 BSE micrographs of the solution-treated alloys taken perpendicular to the extrusion direction: (a) ZM81, (b, d) ZM81-4Sn, and (c) ZM81-8Sn

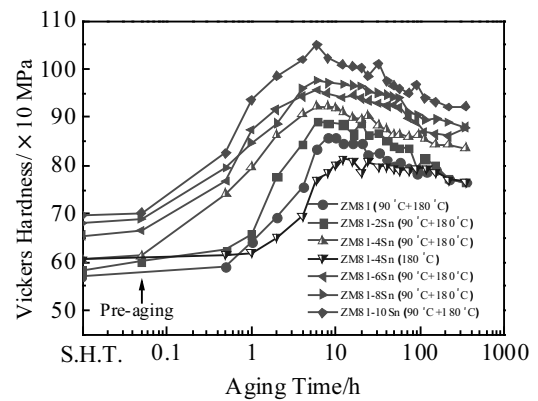


Fig.10 Aging curves of the solution-treated alloys subjected to single aging at 180 °C and double aging at 180 °C (pre-aging at 90 °C for 24 h and second aging at 180 °C)

increase with increasing the Sn content, while the time to reach the peak hardness is almost the same.

The purpose of solution treatment is to obtain a super-saturated solid solution state, which is prepared for the subsequent aging treatment. Fig.11a shows a bright-field (BF) TEM micrograph of ZM81-4Sn in the solution-treated state. Based on XRD result and EDS analysis, only pure Mn

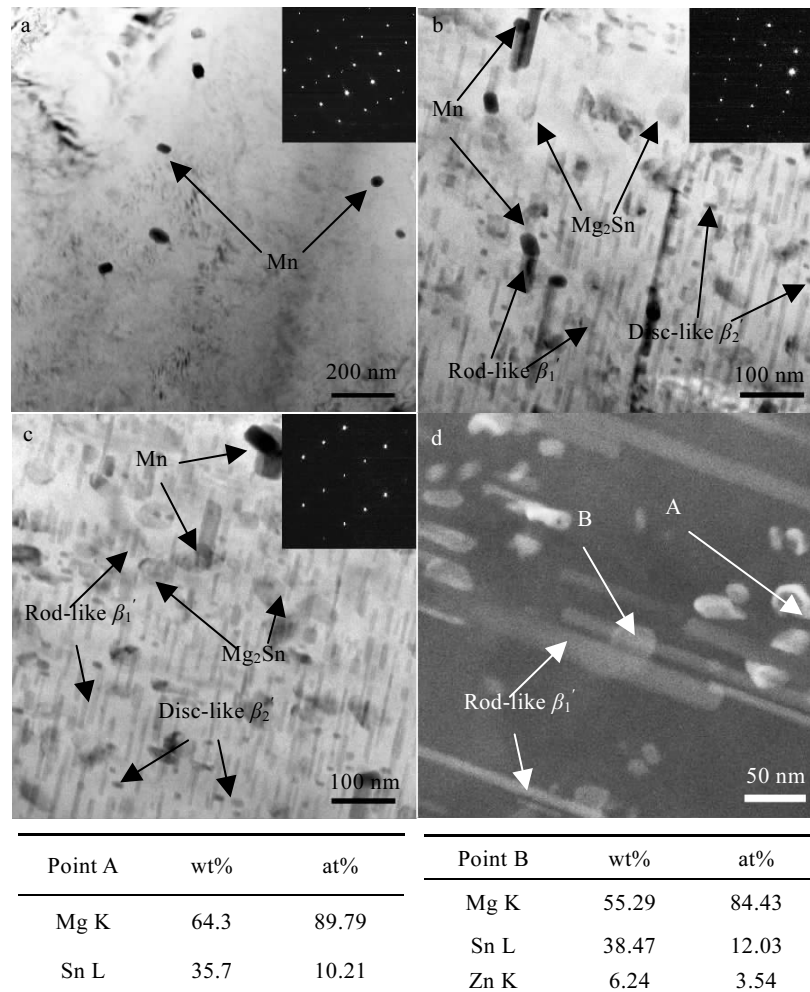


Fig.11 BF-TEM image of solution-treated ZM81-4Sn alloys taken along the  $[1\bar{2}1\bar{3}]$  zone axis of the Mg matrix (a); BF-TEM image of peak-aged ZM81-4Sn alloys by single aging (b) and double aging (c) taken along the  $[01\bar{1}0]$  zone axis; HAADF-STEM image of peak-aged alloys by single aging (d); corresponding EDS results of point A and point B in Fig.11d

phase can be observed. The morphologies of Mn phases include spherical-shape, polygon and rod, which have two orientation relationships with the Mg matrix, as reported in our previous study<sup>[17]</sup>. After T6 treatments,  $MgZn_2$  and  $Mg_2Sn$  precipitates are formed in the ZM81-4Sn alloy, as illustrated by XRD patterns in Fig.7 (peak aged by single aging). Fig.11b and 11c show the BF-TEM micrographs of ZM81-4Sn alloys subjected to peak aging by single (180 °C/12 h) and double aging (90 °C/24 h+180 °C/6 h), respectively. The images are obtained from the  $[01\bar{1}0]$  zone axis. In both states, the peak-aged samples have four kinds of second phase particles. One is pure Mn particles, which are formed and dispersed in the matrix during the smelting and casting stage. It can be seen that the Mn particles can act as the nucleation core of  $\beta_1'$  precipitate during aging treatment, which has been proven in our previous re-

searches<sup>[18]</sup>. The other three second phases are the precipitates during the aging treatment. One is rod along the  $[0001]$  direction of the matrix. The second is on the (0001) basal plane, considered to be transition rod-like  $\beta_1'$  and disc-like  $\beta_2'$  phases ( $MgZn_2$ )<sup>[5, 17]</sup>. The interface between  $\beta_1'$  and the matrix is coherent, while it is semi-coherent between  $\beta_2'$  and the matrix. So the  $\beta_1'$  precipitate can act as a more enormous impediment to the motion of dislocations than  $\beta_2'$  precipitate<sup>[5]</sup>. The third precipitate is an uncommon morphology. Fig.11d shows a high-angle annular dark-field scanning transmission electron microscope (HAADF-STEM) micrograph of alloys in the single aged state. As shown in Fig.11, EDS results indicate that the third phase is Sn-rich precipitate, which is  $Mg_2Sn$  phase confirmed by XRD analysis. Most of the irregular  $Mg_2Sn$  precipitates are flaky-like, not consistent with known

Mg-Sn phases<sup>[9]</sup>. Detailed TEM analysis is underway to identify its nature. In addition, the precipitates after double aging are much finer and far more homogeneously distributed than those after single aging, and a large number of Mg<sub>2</sub>Sn precipitates are homogeneously dispersed among the rod-like β<sub>1</sub>' precipitates.

**2.4 Mechanical properties**

Fig.12 shows the mechanical properties of the ZM81-xSn alloys in the as-extruded and peak-aged conditions. Combined with our previous studies<sup>[6, 19]</sup>, it can be seen that Sn addition results in a beneficial effect on improving the mechanical properties of the as-extruded and peak-aged ZM81 alloys. In the as-extruded condition (Fig.12a), the elongation decreases gradually while the ultimate tensile strength (UTS) and 0.2% yield strength (YS) increase with increasing the Sn content. The as-extruded ZM81-4Sn alloy, which has the optimal mechanical properties, exhibits the UTS of 348 MPa, the YS of 265 MPa and the elongation of 10.38%. The strength is even higher than that of commercially available high-strength Mg-Zn-Zr and Mg-Al-Zn wrought alloys in the as-extruded condition<sup>[20]</sup>. As shown in Fig.12b and 12c, T6 treatments result in a large increase in YS and UTS of all the alloys as compared with as-extruded condition. On the one hand, with increasing the Sn content, the elongation decreases gradually while the UTS and YS significantly increase, and the maximum strength is obtained for the alloy containing 4 wt% Sn. Further increase in Sn content results in a slight reduction of UTS and YS in the peak-aged conditions. On the other hand, the strength of the double aged samples is higher than that of the single aged ones, while the elongation is slightly lower. The mechanical properties of the double aged ZM81-4Sn alloy are the UTS of 416 MPa, YS of 393 MPa and elongation of 4.1%, while those of single aged sample are the UTS of 406 MPa, YS of 381 MPa and elongation of 5.38%. The strength is comparable to that of some T5-treated or T6-treated RE-containing Mg alloys<sup>[21]</sup>.

The high strength of the as-extruded ZM81-xSn alloy is mainly determined by grain refinement strengthening. It is well-known that strengthening via grain size control is particularly effective for Mg alloys because of the higher Hall-Petch coefficient<sup>[22]</sup>. With an increase in the Sn content, grain size becomes much smaller by grain broken during deformation. More abundant Mg<sub>2</sub>Zn<sub>3</sub> and Mg<sub>2</sub>Sn particles are dynamically formed during extrusion, which results in a reduction in the size of recrystallized grains through effective inhibition of their growth via the grain boundary pinning effect. The tensile strength and compressive yield strength of the extruded alloy are improved gradually with an increase in the Sn content, which is mainly attributed to the enhancement of the grain boundary hardening. The high strength of the peak-aged ZM81-xSn alloy is mainly determined by the combined precipitation strengthening of

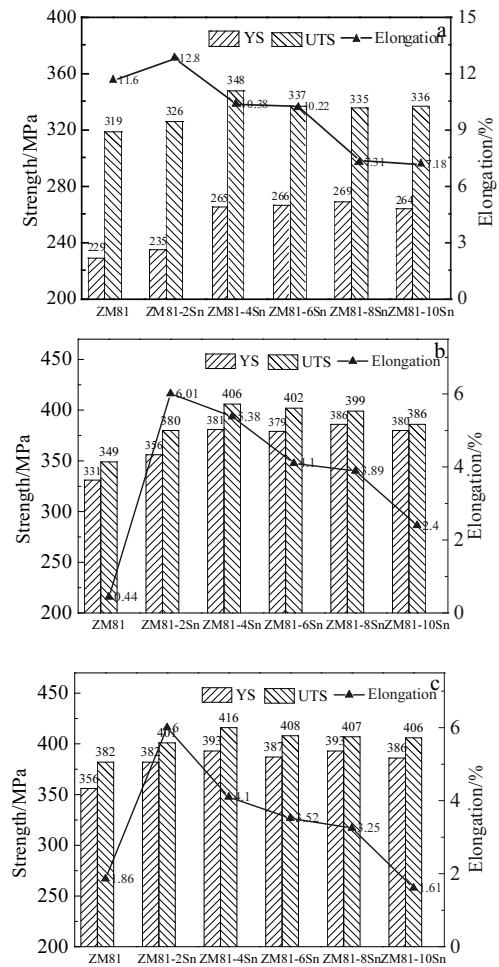


Fig.12 Mechanical properties of the as-extruded (a), single peak aged (180 °C/12 h) (b), and double peak aged (90 °C/24 h +180 °C/6 h) (c) alloys

MgZn<sub>2</sub> and Mg<sub>2</sub>Sn precipitates. As shown in Fig.12, the strength of the as-extruded alloys is increased significantly by the T6 aging treatments. After T4 treatment, almost all the Mg-Zn and Mg-Sn compounds in the as-extruded ZM81-4Sn are dissolved into the matrix, which suggests that a uniform and supersaturated solid-solution structure is produced, as shown in Fig.8c and Fig.9b. Aging treatment for the solution-treated samples is necessary so the finely dispersed β<sub>1</sub>', β<sub>2</sub>' and Mg<sub>2</sub>Sn precipitates form within the grains. The precipitate particles act as obstacles to dislocation movement, thereby strengthening the aged alloy. Moreover, due to the much finer and far more homogeneously distributed precipitates, the strength of the double aged samples is higher than that of the single aged ones.

**3 Conclusions**

1) The microstructure and mechanical properties of the new experimental ZM81 alloys with different Sn contents

subjected to the extrusion, single aging and double aging are investigated. It is found that T6 treatments can markedly improve the strength of as-extruded alloy, and the precipitate strengthening effect of double aging is better than that of single aging. Among them, the ZM81-4Sn alloy with double aging after solution treatment exhibits the highest strength and moderate elongation, i.e., UTS of 416 MPa, YS of 393 MPa and elongation of 4.1%.

2) The high strength of the peak aged alloys is mainly determined by combined precipitation strengthening of the MgZn<sub>2</sub> and Mg<sub>2</sub>Sn precipitates, and the precipitates of the double aged samples are much finer and far more homogeneously distributed than those of single aged ones.

## References

- 1 Ren Lingbao, Fan Lingling, Zhou Mingyang et al. *International Journal of Lightweight Materials and Manufacture*[J], 2018, 1(2): 81
- 2 Zhang Jinghuai, Liu Shujuan, Wu Ruizhi et al. *Journal of Magnesium and Alloys*[J], 2018, 6(3): 277
- 3 Clark J B. *Acta Metallurgica*[J], 1965, 13(12): 1281
- 4 Langelier B, Sha G, Korinek A et al. *Materials & Design*[J], 2017, 119: 290
- 5 Oh-Ishi K, Hono K, Shin K S. *Materials Science and Engineering A*[J], 2008, 496(1-2): 425
- 6 Zhang Dingfei, Shi Guoliang, Xia Bingzhao et al. *Transactions of Nonferrous Metals Society of China*[J], 2011, 21(1): 15
- 7 Yu Daliang, Zhang Dingfei, Sun Jing et al. *Journal of Alloys and Compounds*[J], 2017, 690(5): 553
- 8 Mendis C L, Bettles C J, Gibson M A et al. *Materials Science and Engineering A*[J], 2006, 435: 163
- 9 Liu Chaoqiang, Chen Houwen, Nie Jianfeng. *Scripta Materialia*[J], 2016, 123: 5
- 10 Planken J Van Der. *Journal of Materials Science*[J], 1969, 4(10): 927
- 11 Sasaki T T, Oh-Ishi K, Ohkubo T et al. *Materials Science and Engineering A*[J], 2011, 530: 1
- 12 Qi F G, Zhang D F, Zhang X H et al. *Journal of Alloys and Compounds*[J], 2014, 585: 656
- 13 Wang Yongjian, Peng Jian, Zhong Liping. *Journal of Alloys and Compounds*[J], 2018, 744: 234
- 14 Kim Sang-Hoon, Lee Jong Un, Kim Ye Jin et al. *Journal of Alloys and Compounds*[J], 2018, 751: 1
- 15 Effenberg G, Aldinger F, Rokhlin L. *Ternary Alloys*[M]. Stuttgart: MSI, 1999
- 16 Agarwal R, Fries S G, Lukas H L et al. *Zeitschrift fur Metallkunde*[J], 1992, 83(4): 216
- 17 Shi G L. *Research on Strengthening Mechanism of Mg-Zn-Mn Wrought Magnesium Alloys*[D]. Chongqing: Chongqing University, 2011 (in Chinese)
- 18 Qi F G, Zhang D F, Zhu Z T et al. *Materials Science and Technology*[J], 2012, 28(12): 1426
- 19 Zhang Dingfei, Zhao Xiabing, Shi Guoliang et al. *Rare Metal Materials and Engineering*[J], 2011, 40(3): 418 (in Chinese)
- 20 Polmear I J. *Light Alloys*[M]. Amsterdam: Elsevier, 2005: 237
- 21 Pan Hucheng, Ren Yuping, Fu He et al. *Journal of Alloys and Compounds*[J], 2016, 663: 321
- 22 Bae Sang Woo, Kim Sang-Hoon, Lee Jong Un et al. *Journal of Alloys and Compounds*[J], 2018, 766: 748

## ZM81-xSn 变形镁合金的组织演变和力学性能

齐福刚<sup>1,2</sup>, 罗文忠<sup>2</sup>, 吴传平<sup>1</sup>, 赵 镡<sup>1,2</sup>, 叶芝松<sup>2</sup>, 侯彩红<sup>1</sup>, 张丁非<sup>3</sup>

(1. 电网输变电设备防灾减灾国家重点实验室, 湖南 长沙 410000)

(2. 湘潭大学, 湖南 湘潭 411105)

(3. 重庆大学, 重庆 400045)

**摘要:** 通过对不同 Sn 含量 ZM81 合金的微观组织和力学性能表征, 研究了 Sn 在 ZM81 合金中的存在形式和作用机制及不同添加量对合金显微组织和力学性能的影响。结果表明: Sn 元素主要以 Mg<sub>2</sub>Sn 共晶相形式存在, 能够细化铸态组织; 热挤压过程中, Sn 添加能够起到抑制动态再结晶和晶粒细化的作用; T6 处理, 尤其是双级时效, 能显著提升挤压态合金的力学性能, 其中 ZM81-4Sn 合金具有最佳综合力学性能, 其抗拉强度、屈服强度和延伸率分别为 416 MPa、393 MPa 和 4.1%。实验合金高强度主要源于 MgZn<sub>2</sub> 和 Mg<sub>2</sub>Sn 析出相的双重时效强化效果; 相比单级时效, 双级时效态合金的析出相更细小弥散, 因此其力学性能更优。

**关键词:** ZM81合金; Sn; 析出相; 力学性能

作者简介: 齐福刚, 男, 1986 年生, 博士, 副教授, 湘潭大学材料科学与工程学院, 湖南 湘潭 411105, 电话: 0731-58298119, E-mail: qifugang@xtu.edu.cn